Journal of Applied Engineering and Technological Science
Vol 7(1) 2025: 550-568

DEVELOPING A COST-EFFECTIVE AIR QUALITY MONITORING SOLUTION USING IOT TECHNOLOGY: ADDRESSING LONG-DISTANCE TRANSMISSION CHALLENGE

Jarun Khonrang[1], Seksan Winyangkul[2], Pairoj Duangnakhorn[3], Rungrat Viratikul[4], Kamol Boonlom[5]*

Faculty of Industrial Technology, Chiangrai Rajabhat University, Chiangrai, Thailand[1235]
Department of Electrical Engineering, Faculty of Engineering, Chulalongkorn University, Thailand [4]
jarun.kho@crru.ac.th[1], seksan.win@crru.ac.th[2], pairoj.dua@crru.ac.th[3], 6571022121@student.chula.ac.th[4], kamol.boo@crru.ac.th[5]

Received: 06 October 2024, Revised: 26 August 2025, Accepted: 10 September 2025
**Corresponding Author*

ABSTRACT
This research explores the integration of Internet of Things (IoT) technology and LoRa repeaters to enhance air quality monitoring. IoT enables low-cost, real-time sensors for continuous air quality assessment, while repeaters address the limitations of traditional wireless communication over long distances. Our study demonstrates the effectiveness of a LoRa repeater system, with signal strengths between monitoring stations and repeaters ranging from -84 dBm to -92 dBm, achieving a practical operational range of 850 meters. The highest Packet Delivery Ratio (PDR) recorded was 65% using a Spreading Factor (SF) of 10, while SF 7 resulted in a PDR of 25%. Environmental factors and antenna gain were identified as critical for optimizing transmission power and communication reliability. This research underscores the potential of advanced IoT applications in extending internet connectivity and improving air quality management across various sectors, paving the way for smarter urban environments and public health initiatives.
Keywords : *LoRa Mesh Network, Wireless Internet of Things Technology (WIoT), Air Quality Monitoring.*

1. Introduction

Air pollution poses serious global and local challenges, contributing to millions of premature deaths annually and imposing substantial economic burdens on governments and industries. Globally, ambient air pollution accounts for more than 3.2 million premature deaths each year (Cohen et al., 2017). In Thailand, PM2.5 levels exceeded the World Health Organization's guideline fourfold in 2022, leading to over 33,000 premature deaths and an economic loss of approximately 2.17 trillion baht, or 11% of the national GDP (Greenpeace Southeast Asia, 2022). In the European Union, the industrial sector incurs costs estimated between 59 and 189 billion euros annually due to air pollution (European Environment Agency, 2021). Indoor air pollution is equally concerning, contributing to more than 4.3 million premature deaths annually, particularly in low- and middle-income countries (World Health Organization, 2021). These health and economic impacts underscore the urgent need for continuous and reliable air quality monitoring (Hossain & Muhammad, 2016; Adelantado et al., 2017).

Traditional monitoring systems are often expensive, location-limited, and labor-intensive, restricting their scalability and limiting their use in real-time applications (Industrial Air Pollution, 2014). To overcome these challenges, the Internet of Things (IoT) has emerged as a transformative solution, enabling the deployment of cost-effective, low-power sensors for distributed and continuous monitoring of air pollutants. IoT systems facilitate real-time data collection, raise public awareness, and support data-driven environmental management strategies that are critical for developing smart cities and sustainable communities (Zanella et al., 2014). However, their effectiveness depends on the underlying communication technologies, which face significant technical limitations. Conventional wireless protocols such as Wi-Fi, Bluetooth, and ZigBee are optimized for short-range connectivity and often fail to deliver reliable long-distance transmission required in large-scale monitoring networks (Shafique et al., 2020). Even with low-power wide-area network (LPWAN) technologies such as LoRa, NB-IoT, and Sigfox, ensuring

stable performance across diverse terrains and obstructed urban environments remains a challenge (Sha et al., 2018).

To address this gap, this study proposes a LoRa repeater system to extend the transmission range of IoT-based air quality monitoring stations. Repeaters serve as intermediaries that receive, amplify, and retransmit signals, improving coverage, reducing data loss, and maintaining stable connectivity where direct communication is unreliable (Ndaguba et al., 2023). Unlike conventional star-topology approaches, the proposed design applies a mesh-inspired configuration that minimizes interference and enhances packet delivery by separating frequency channels for upstream and downstream communication. Specifically, the repeater receives data from the monitoring station at 923.2 MHz and retransmits it to the gateway at 923.4 MHz, thereby reducing inter-channel interference and optimizing throughput.

The main contributions of this study are threefold. First, it presents the design and implementation of a cost-effective IoT-based air quality monitoring system integrated with LoRa repeaters. Second, it evaluates system performance in terms of Received Signal Strength Indicator (RSSI), Packet Delivery Ratio (PDR), and effective transmission distance under real-world conditions. Third, it analyzes the trade-offs between spreading factor, bandwidth, and system reliability to provide guidelines for practical deployments. By addressing the limitations of long-distance communication in IoT-based monitoring, this work advances scalable and reliable solutions for air quality management in both urban and semi-rural environments (Boonlom et al., 2024; Morawska et al., 2018).

2. Literature Review

Poor air quality has been shown to pose severe risks to human health worldwide. Exposure to air pollutants significantly increases the incidence of respiratory and cardiovascular diseases, with vulnerable groups such as children, the elderly, and individuals with pre-existing conditions disproportionately affected (Brunekreef & Holgate, 2002; World Health Organization, 2021). Globally, air pollution contributes to approximately 3.2 million premature deaths annually (Cohen et al., 2017). In Thailand, PM2.5 levels exceeded WHO guidelines fourfold in 2022, causing more than 33,000 premature deaths and economic losses equivalent to 11% of national GDP (Greenpeace Southeast Asia, 2022). These figures underscore the urgent need for robust monitoring solutions (Lin et al., 2017).

The economic burden of air pollution is equally significant. In the European Union, the industrial sector alone incurs annual costs ranging from 59 to 189 billion euros due to pollution-related impacts (European Environment Agency, 2021). Such economic and health challenges highlight the necessity of continuous air quality assessment systems to inform public health policies and mitigate long-term societal costs (Popoola et al., 2018).

Indoor air pollution (IAQ) is an additional and often underestimated concern. Pollutants from domestic cooking and heating, especially in low- and middle-income countries, frequently lead to indoor concentrations exceeding outdoor levels (World Health Organization, 2021). Globally, IAQ is responsible for more than 4.3 million premature deaths each year. This disproportionate impact reinforces the demand for affordable and scalable monitoring systems capable of capturing both outdoor and indoor pollution dynamics (Castell et al., 2017).

Traditional monitoring approaches, which rely on manual sampling or high-cost equipment, provide limited spatial and temporal resolution (Industrial Air Pollution, 2014). These methods are unsuitable for real-time applications and cannot easily be scaled to cover large urban or rural areas. To overcome such limitations, the Internet of Things (IoT) has emerged as a transformative solution. IoT enables deployment of distributed, low-cost sensors capable of real-time air quality monitoring, thereby enhancing data availability and enabling data-driven management strategies (Zanella et al., 2014). IoT-based monitoring has already been deployed in applications ranging from smart cities to precision agriculture, demonstrating the scalability and adaptability of the approach (Kitchin, 2014).

Despite these advantages, IoT-based monitoring systems face communication challenges. Conventional wireless technologies such as Wi-Fi, Bluetooth, and ZigBee are limited to short ranges (typically <200 m) and suffer from high energy consumption and interference in dense deployments (Shafique et al., 2020). To address these shortcomings, low-power wide-area

network (LPWAN) technologies have been developed, including Narrowband IoT (NB-IoT), LTE-M, Sigfox, and LoRa. NB-IoT and LTE-M, which operate in licensed spectrum, provide high reliability and wide coverage but involve higher costs and operator dependence. Sigfox offers low-cost ultra-narrowband connectivity but is limited by low data rates and coverage constraints (Adelantado et al., 2017). In contrast, LoRa operates in unlicensed spectrum, offering long-range (up to 10 km in rural areas), low power consumption, and cost-effective deployment, making it particularly suitable for environmental monitoring applications (Qadir et al., 2018; Viratikul et al., 2024; Belli et al., 2015; Li et al., 2015).

Nevertheless, LoRa's single-hop star topology suffers performance degradation in obstructed urban or underground environments, and its range is often shorter than theoretical limits (Duong et al., 2018). Several solutions have been explored to address these limitations. Duong et al. (2018) proposed multi-hop LoRa protocols for linear infrastructures such as pipelines and power lines, though their method lacked downlink capability. Abrardo and Pozzebon (2019) optimized multi-hop LoRa for underground aqueducts, showing that while range could be extended, energy consumption increased due to synchronization requirements. Satellite communication has also been considered for IoT backhaul, but high costs and energy demands make it impractical for low-cost air quality monitoring (Ndaguba et al., 2022; Magno & Benini, 2014).

Repeaters provide a promising alternative by extending LoRa's communication range without requiring complex synchronization protocols. By receiving, amplifying, and retransmitting signals, repeaters can mitigate packet loss and maintain stable connections in obstructed environments. Recent studies have shown that repeater-enhanced LoRa systems improve coverage and reliability while maintaining energy efficiency (Boonlom et al., 2024a; Boonlom et al., 2022). Compared to multi-hop or satellite solutions, repeaters offer a simpler and more cost-effective strategy for ensuring long-distance connectivity in IoT-based monitoring networks (Ksentini & Nikaein, 2017).

In summary, the reviewed literature highlights the urgent need for reliable and scalable long-distance IoT communication in air quality monitoring. Traditional methods are costly and limited in scope, while conventional wireless protocols lack sufficient range. LPWAN technologies such as LoRa, NB-IoT, and Sigfox each offer trade-offs, but LoRa presents the best balance of cost, range, and energy efficiency. Its limitations at long distances, however, necessitate enhancement through repeater-based architecture. This study directly addresses this research gap by designing and evaluating a LoRa repeater system for air quality monitoring, aiming to provide a cost-effective, scalable, and reliable solution for real-world deployments.

3. Research Materials and Methods

This study develops a cost-effective long-range data transmission system for air quality monitoring using LoRa (Long Range) technology enhanced with repeater nodes. LoRa was selected as the transmission technology due to its favorable balance of long-range communication, low power consumption, and cost-effectiveness compared to alternatives such as Wi-Fi, ZigBee, NB-IoT, and Sigfox. While NB-IoT and LTE-M operate in licensed spectrum and provide high reliability, they incur subscription costs and require extensive infrastructure. Sigfox offers low-cost connectivity but has strict bandwidth limitations. In contrast, LoRa operates in unlicensed spectrum and supports distances up to 10 km in rural settings, making it particularly suitable for environmental monitoring where cost and scalability are critical (Qadir et al., 2018; Vijay et al., 2023; Boonlom et al., 2025; Boonlom et al., 2021).

3.1 Overview of the LoRa Mesh Internet of Things

The Internet of Things (IoT) connects physical devices for real-time monitoring and control, creating demand for communication technologies that are energy-efficient and support long-distance transmission. Traditional protocols such as Wi-Fi and ZigBee provide high data rates but are limited in range, making them unsuitable for large-scale deployments. To address this, Low Power Wide Area Network (LPWAN) technologies were developed, including licensed solutions (NB-IoT, LTE-M) and unlicensed solutions (Sigfox, LoRa).

This study focuses on LoRa (Long Range), which offers extended coverage (up to 10 km in rural areas), low power consumption, and low cost compared to alternatives. LoRa's chirp spread spectrum modulation provides robust performance in noisy or obstructed environments, making it well-suited for environmental monitoring.

For this research, LoRa is applied to air quality monitoring, with data from distributed sensor nodes transmitted via repeater-based architecture. As shown in Fig. 1, the repeater relays signals between the monitoring station and the gateway, extending coverage beyond conventional single-hop LoRa networks. Powered by solar energy with battery backup, the system ensures sustainable, autonomous operation in remote areas.

This approach combines IoT, LPWAN, and renewable energy to deliver a cost-effective and reliable monitoring solution that improves pollutant detection accuracy while supporting public health awareness and smart city development.

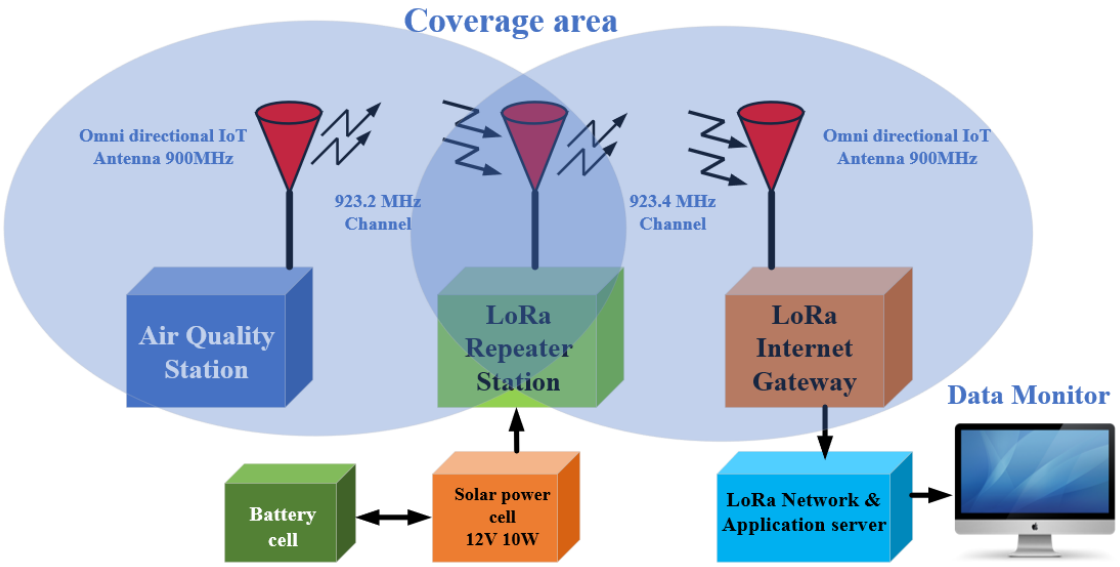

Fig. 1. The functional schematic of a repeater system LoRa is intended for use in research.

3.2 Hardware Design

The proposed IoT-based air quality monitoring system consists of three main elements: (1) an air quality monitoring node, (2) a LoRa repeater, and (3) a gateway. Together, these components form a cost-effective, low-power architecture capable of transmitting data reliably over extended distances.

- Air Quality Monitoring Node

The air quality monitoring station, illustrated in Fig. 2, is built around an Arduino Mega 2560 microcontroller, selected for its multiple I/O interfaces and compatibility with diverse environmental sensors. The system integrates a set of gas and particulate sensors designed to measure different air quality parameters under varying conditions, including MQ-9 (CO), MG-811 (CO_2), MQ-131 (O_3), 2SH12 (SO_2/NO_2), and PMS3003 (PM2.5 and PM10), which are detailed in Table 1. Sensor selection was guided by critical criteria such as high accuracy, low energy consumption, and suitability for long-term monitoring applications. For gaseous pollutants, individual electrochemical sensors with separated electrodes were employed instead of multi-electrode configurations, as the latter often compromise measurement precision. For particulate matters, laser-based scattering technology was implemented to enable precise and real-time detection of airborne dust particles. The sensors interface with the microcontroller via a 12-bit analog input for gas measurements, while particulate matter data are transmitted through a USART interface, ensuring accurate and efficient data acquisition.

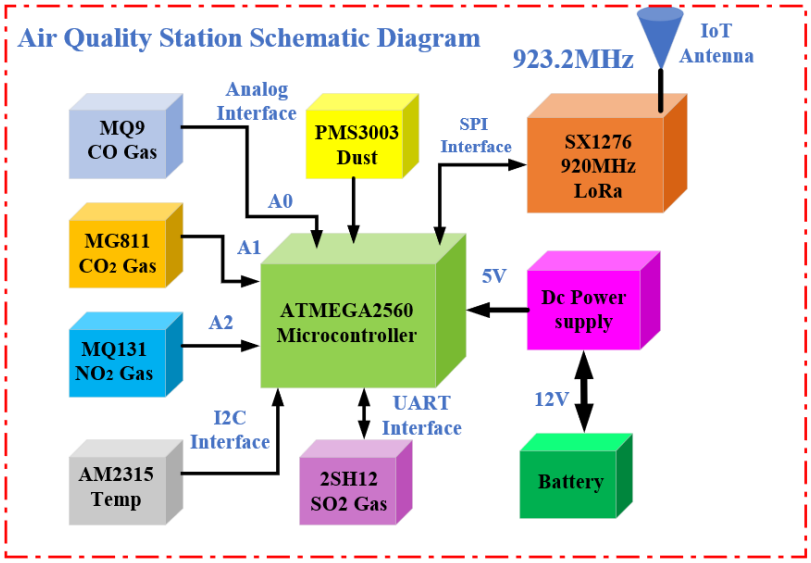

Fig. 2. Illustration of an air quality sensor node for research applications.

Table 1 - The characteristics of the sensors

Gas Sensors				
Sensor	Target Gas	Range (ppm)	Resolution(ppm)	Response Time (seconds)
MQ-9	CO	100 to 10000ppm	10 to 1000ppm	<60s
MG-811	CO_2	350 - 10,000ppm	10 to 1000ppm	<60s
MQ-131	NO_2	10 ~ 1000 ppm	10ppb – 2ppm	<100s
2SH12	SO_2	1 to 500ppm	1-500ppm	≤30S
AM2315C	Temp & Humidity	-20 to 80°C	0-100% humidity	
Particulate Matter				
Sensor	sensor type	Range (um)	Resolution(ug/m3)	Response Time (seconds)
PMS3003 Laser Dust	PM2.5	0 - 500	1	<10s
Sensor	PM10	0 - 500	1	<10s

- The LoRa Repeater

For wireless communication, the monitoring node is equipped with an SX1276 LoRa transceiver module, which operates in the 923 MHz ISM band and supports chirp spread spectrum modulation with adjustable spreading factors. This configuration enables long-range, low-power communication, making it well-suited for continuous real-time monitoring in outdoor environments. To address the range limitations of single-hop LoRa transmission, a repeater node was developed. The repeater, illustrated in Fig. 3, employs an Arduino Nano microcontroller connected to two SX1276 modules via SPI communication. One module receives signals from the monitoring node at 923.2 MHz, while the other retransmits them to the gateway at 923.4 MHz, thereby reducing interference and minimizing the likelihood of packet collisions. Given that many deployment sites are remote and lack access to grid power, the repeater incorporates solar panels with backup battery storage to maintain autonomous operation. This design takes advantage of LoRa's inherently low power consumption, ensuring reliable, sustainable performance under real-world conditions. The detailed configuration parameters of the LoRa communication system are summarized in Table 2.

- Gateway

The gateway is implemented using a Raspberry Pi with a LoRaWAN concentrator. It receives retransmitted data from the repeater and forwards it to the ThinkSpeak IoT platform via cellular internet. This enables cloud-based storage, processing, and real-time visualization of air quality data through an online dashboard.

This integrated hardware configuration ensures accurate sensing of pollutants, reliable long-distance data transmission via repeaters, and centralized data availability for analysis and decision-making.

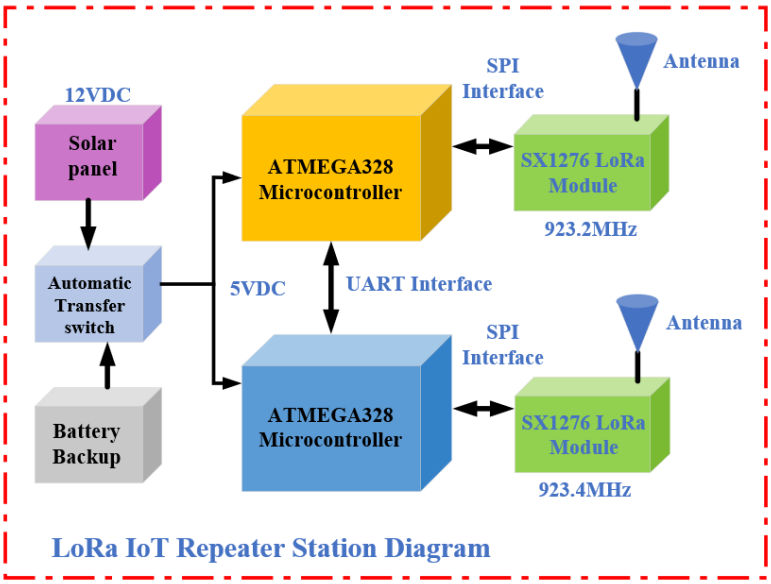

Fig. 3. Connectivity schematic of the LoRa repeater.

Table 2 - depicts the parameter setting of the LoRa.

Parameters	Configuration
Bandwidth(BW)	125kHz
Node transmitting power.	20dBm
Repeater transmitting power	20dBm
Node spreading factor (SF)	7
Repeater spreading factor (SF)	7
Node to Repeater Frequency Channel	923.2MHz
Repeater to Gateway Frequency Channel	923.4MHz
Antenna gain	3dBi
Transmit time interval	1 Second
Node to repeater Tx/Rx height	1.7 meters
Repeater to gateway to repeater Tx/Rx height	1.7 meters

4. Implementation

- The measurement setup and procedure for LoRa point-to-point communication

LoRa employs spread-spectrum modulation to establish connectivity, utilizing a chirp spread spectrum (CSS) technique that modulates symbols across a fixed bandwidth through the use of chirps. The spreading factor (SF) plays a critical role in this process; it dictates the number of chirps used, and increasing the SF can enhance the communication range. However, this increase comes at a cost, as higher SF values lead to a reduction in data rate and an extension of transmission duration, which in turn increases energy consumption. The modulation technique inherent in LoRa allows for an optimal balance between range and energy efficiency by adjusting the spreading factor (SF) (Qadir et al., 2018; Akyildiz & Jornet, 2010).

Table 3 - The LORA Demodulator's Sensitivity (BW 125 kHz) is presented in RSSI and SNR.

Spreading factor	RSSI (dBm)	SNR(dB)
SF6	-118	-5
SF7	-123	-7.5
SF8	-126	-10
SF9	-129	-12.5
SF10	-132	-15
SF11	-133	-17.5
SF12	-136	-20

To facilitate the seamless installation of peer-to-peer (P2P) links, the nodes can be affixed to the wall of the air quality monitoring station at a convenient height of 1.7 meters, as illustrated in Fig. 4. The anticipated transition of LoRa point-to-point links into a mesh network is expected

to yield similar advantages regarding ease of deployment and flexibility. A platform based on a LoRa modem has been developed, incorporating open-source hardware, including the SX1276, along with corresponding software, to enhance reproducibility (Khonrang et al., 2023; Boonlom et al., 2023). This setup will support the experimental findings effectively.

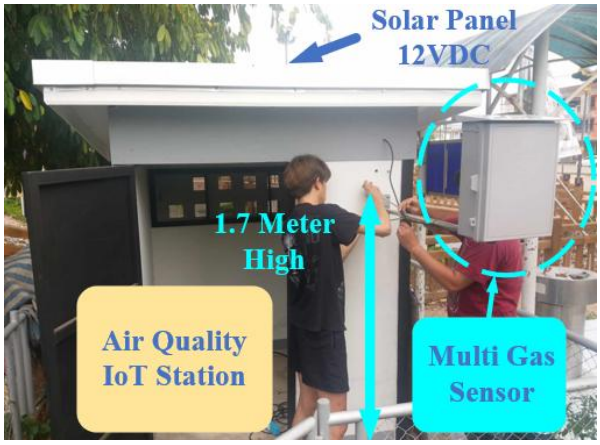

Fig. 4. The installation site of the LoRa node air quality station is shown.

We have established an experimental setup featuring short antennas and receivers, tailored to simulate scenarios requiring basic antenna and gateway configurations. The aim of the point-to-point communication experiment is to ascertain the maximum transmission range of the LoRa module. The LoRa air quality sensor node will be permanently installed at the designated location of the measuring station, while the LoRa test node will be moved away from the sensor node to evaluate the received signal strength indicator (RSSI) and determine the maximum transmission distance.

Path loss calculations are utilized to estimate potential signal degradation, and the minimum received signal level over various distances. The installation site for line-of-sight calculations is situated in an open area, where environmental factors play a significant role. Path loss models serve to predict the reduction in signal power as it propagates through different media, accounting for phenomena such as wave expansion, reflection, scattering, diffraction, and absorption. The overall path loss is influenced by environmental conditions, as well as the distances and heights of the transmitting and receiving antennas. It is important to note that the parameters of the path loss model typically apply only within specific frequency ranges, antenna configurations, and environmental settings. The conventional path loss (PL) model is characterized by a logarithmic power law that includes a random component (Olasupo et al., 2016). Equation (1) illustrates the log-distance path loss model expressed in decibels (dB).

$$path_{loss_m}(d) = PL(d_0) + 10nlog_{10}\left(\frac{d}{d_0}\right) + X\sigma, d \geq d_0 \quad (1)$$

In this context, n denotes the path loss exponent, while d signifies the distance, measured in meters, between the receiver and transmitter. The term $x\sigma$ refers to the variability observed around the average value. Where, $N\left(0, \sigma^2\right)$ is a model used to represent large-scale fading. While $PL(d_0)$ is the path loss at a reference distance of d_0. A reference distance d_0 of 1m was used for the modelling experiments. The estimation of $PL\left(d_0\right)$ is obtained through the fitting method applied to the measured data. In this context, the subscript m denotes the modeled path loss, while s represents the sampled path loss. Moreover, the standard deviation σ can be understood as either a constant scalar value or a variable that varies with distance, as expressed in equation (2). This flexibility in defining the standard deviation allows for a more accurate representation of the path loss characteristics in various scenarios (Boonlom et al., 2009; Jayaraman et al., 2016).

$$\sigma(d) = a log_{10}\left(\frac{d}{d_0}\right) + b \tag{2}$$

The current study employs the LoRa SX1276 wireless data transmission module, which operates at a transmission power of 20 dBm within the frequency bands of 923.2 MHz and 923.4 MHz. The path loss is significantly influenced by the broad angle of wave emission. As distance increases, the strength of the wave signal diminishes due to the dispersion of the wave in free space propagation, as indicated by equation (3).

$$\frac{P_R}{P_T} = G_T G_R \left[\frac{\lambda}{4\pi d}\right]^2 \tag{3}$$

P_R is measuring the signal power unit in (dBm).

P_T is the transmitted power in decibels (dBm).

G_R refers to the unit of receiver an antenna expansion, dBi.

G_T is an expanded rate of the sender an antenna unit, dBi.

λ is the wavelength value, which $\lambda = c/f$.

C is light speed $(3 \times 10^8 m/s)$.

f is the signal frequency unit (hertz).

d denotes the distance, measured in meters, between the receiving and transmitting portions.

Consequently, the attenuation of signal strength in the air is measured in decibels (dB) according to equation (4) (Kumar et al., 2016).

$$L_{dB} = 10\log(P_T) - 10\log(P_R) \tag{4}$$

When choosing an antenna for signal transmission and reception, it is crucial to employ identical antenna types, particularly a monopole antenna with power gain capabilities, rated at 3 dBi. The parameters are set at PT = 20 dBm, and both the receiver and transmitter gain (GR and GT) are also 3 dBi, with a wavelength (λ) of 0.324 m and a distance of 1 kilometer separating the transmitter from the receiver.

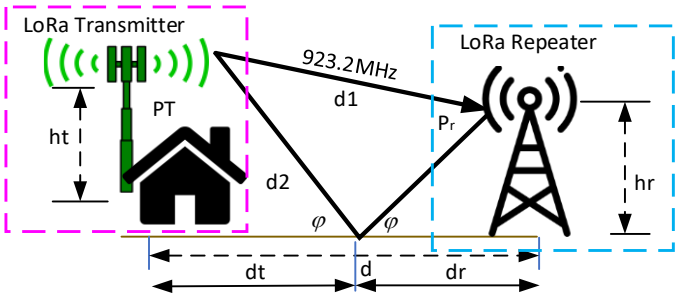

Fig. 5. Presenting the calculation diagram and the architecture of the data transmission system.

Fig. 5. depicts the different paths and distances traveled by the two signals. As a result, when the signals reach the receiving antenna, they may undergo a phase shift. Therefore, it is essential to calculate the difference in distance traveled by the two waves, as detailed in equation (5).

$$\Delta d = d_2 - d_1 = \sqrt{(h_T - h_R)^2 + d^2} - \sqrt{(h_T - h_R)^2 + d^2} \tag{5}$$

The Received Signal Strength Indicator (RSSI) value fluctuates according to the signal strength. A higher RSSI value signifies a closer proximity between the transmitter and receiver, whereas a lower value indicates greater distance between them. This calculation can be conducted using equation (6).

$$RSSI = -10n\,log_{10}\,d + A \tag{6}$$

In this context, n denotes the path loss exponent, typically assigned a value of n=2. The variable d represents the distance between the transmitter and receiver, while A=1 signifies the received power in dBm when antennas are in close proximity. The signal-to-noise ratio (SNR) between the transmitter and receiver is expressed in meters, with the RSSI value measured in dBm. The SNR can be derived from equations (7).

$$SNR = 174 + RSSI - P_{tx} - 10\,log_{10}\,B\,W - NF \tag{7}$$

P_{tx}represent the transmission power of the transmitter, indicates the amplitude of the transmitting frequency measured in kHz, and NF denotes the noise figure for both the transmitter and receiver. Constant 174 refers to the thermal noise, which is dependent on the temperature of the receiver and is calculated based on a bandwidth of 1 Hz.

To test the system, the air quality monitoring station was installed in a specific location within the Mae Chan Sub-district Municipality, Mae Chan District, Chiang Rai Province, as depicted in Fig. 6. A stationary setup was established on the transmission (TX) side, consisting of a single transceiver configured to transmit packets using a spreading factor of 7 (SF7).

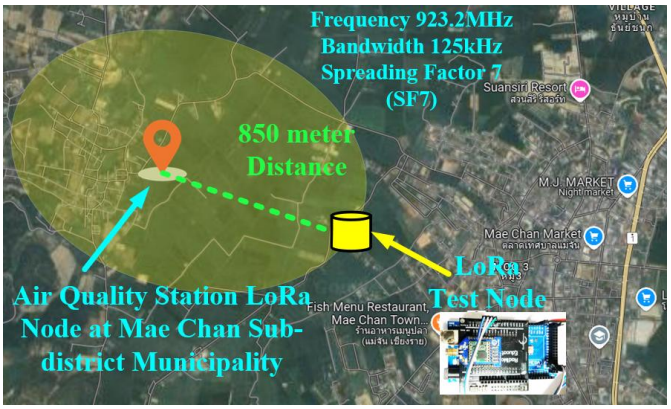

Fig. 6. Illustrates the map and the distance separating the monitoring station from the LoRa test node.

Fig. 6. presents the map illustrating the distance of 850 meters between the air quality monitoring station and the LoRa test node installed in Mae Chan Sub-district Municipality, Chiang Rai Province, Thailand. During the measurement of the Received Signal Strength Indicator (RSSI) value, which was recorded 10 times, the received signal strength averaged approximately -89 dBm.

Fig. 7. displays the LoRa test node board used for measuring the signal strength transmitted by the air quality station's LoRa node. This setup includes the ATMEGA2560 microcontroller connected to the LoRa SX1276 module. At a distance of 850 meters during the experiment, the measured signal level was -89 dBm. It is important to note that this value does not signify the maximum communication distance. In practical scenarios, various factors, such as inclement weather, can contribute to signal attenuation. Nevertheless, the communication system is expected to operate effectively at this distance. To enhance communication, a LoRa repeater will be strategically installed at a point 850 meters away, which represents half the distance between the air quality station's LoRa node and the LoRa gateway.

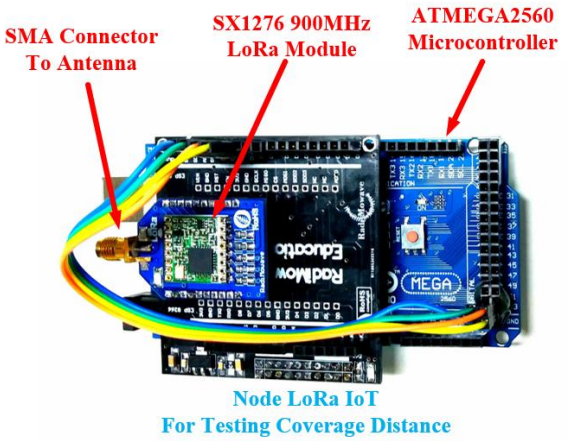

Fig. 7. Depicted LoRa nodes for evaluating signal strength and range.

4.1 The LoRa Mesh Communication Evaluation Configuration

Monitoring systems for linear utilities, such as power lines, waterways, and piping systems, are commonly integrated into Internet of Things (IoT) frameworks. While LoRa technology provides long-range transmission capabilities, its effectiveness diminishes in applications that span over ten kilometers, necessitating the regular placement of gateways. Coverage challenges also arise in underground deployments, such as those in sewage systems and mines. For instance, Duong et al. developed and implemented a multi-hop communication protocol for LoRa networks aimed at extending coverage over long distances . This protocol is particularly suited for linear deployments, such as monitoring gas pipelines or high-voltage lines. In this setup, devices synchronize and activate at predetermined intervals to receive data packets from adjacent devices, which they can then merge with their own and forward to subsequent devices in the network. However, the protocol does not address downlink data transmission.

Additionally, Abrardo, & Pozzebon (2019) developed a multi-hop LoRa linear network tailored for underground settings, with an emphasis on optimizing the sleep and wake cycles of nodes to enhance battery efficiency. Their research revealed that LoRa transmission exhibited a range limitation of approximately 200 meters, rendering the star topology ineffective for monitoring extended aqueducts where line-of-sight was obstructed by curves. To overcome this limitation, the researchers implemented a data propagation model utilizing sensor nodes that create a transmission chain to the gateway. They also integrated a synchronization mechanism to optimize sleep cycle durations during data transmission between node pairs (Jawad et al., 2017).

To address the distance limitations associated with the star topology in LoRa networks, a mesh network configuration has been implemented, which enhances the transmission range within the system. Following the successful design and testing of point-to-point data transmission at a spreading factor (SF) of 7, achieving a transmission distance of 850 meters with an average RSSI value of approximately -89 dBm, it is evident that the chosen SF value is relatively low. The ability of SF 7 to facilitate data transmission over this distance suggests that higher SF values would also be capable of transmitting data effectively. As the spreading factor increases, LoRa supports longer signal reception distances; for example, a higher spreading factor like SF 10 can achieve greater transmission distances compared to lower values such as SF 8. However, it is important to note that increasing the SF will correspondingly decrease the data transmission bandwidth.

In the experimental setup of the LoRa mesh network utilizing a LoRa repeater, multiple transmission frequency bands were employed to mitigate cross-channel interference. This interference often arises from data collisions when two or more devices attempt to transmit simultaneously over a shared network, leading to potential data disruption or loss. The design of the LoRa repeater incorporates two LoRa modules to facilitate a connection between them. Communication between the two ATMEGA328 microcontrollers (specifically Arduino Nano) is accomplished via a serial port, as illustrated in Fig 3. Additionally, Fig. 8. showcases the

operational hardware and installation of the LoRa repeater. This configuration ensures more reliable data transmission and enhances the overall performance of the LoRa network in practical applications .

Fig. 8. The installation site of the LoRa repeater is shown.

During the experimental phase of data transmission from the air quality LoRa station to the gateway, three distinct spreading factor (SF) values—SF 7, SF 9, and SF 10—will be utilized. This methodology aims to evaluate the packet delivery ratio (PDR) and delivery time under varying conditions. The objective is to analyze how the distance between the LoRa repeater and the LoRa gateway influences PDR and delivery time measurements. The experiment involves tracking the movement of a LoRa gateway, which is connected to a cellular internet signal and varies in distance from the LoRa repeater, ranging from 300 meters to 1000 meters. Fig. 9. illustrates the LoRa gateway device used in this investigation. The LoRa modules are tested by transmitting data at a consistent output power level of 20 dBm and a bandwidth of 125 kHz across these different distances.

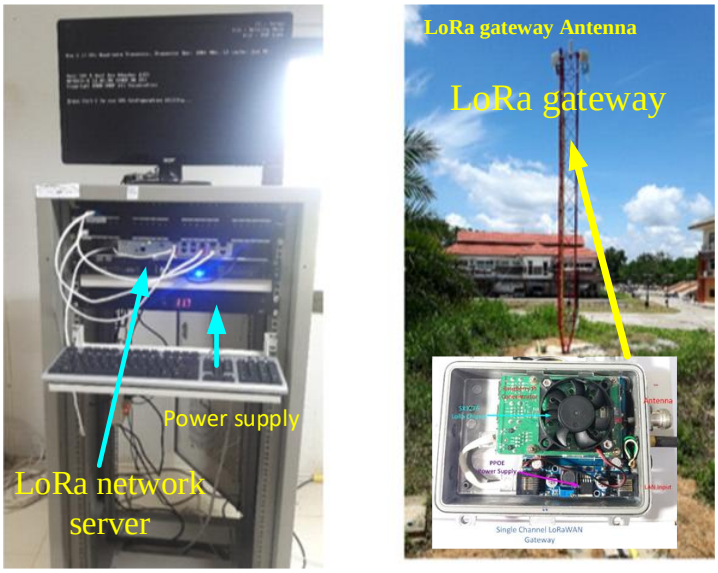

Fig. 9. shows the positioning of the LoRa gateway and LoRa network server during the installation phase.

The system consists of two nodes: an air quality station node and a repeater node, both positioned at a height of 1.7 meters above ground. For optimal performance, the receiver must be aligned in the same unobstructed plane as the transmitter. This experiment evaluated the packet delivery ratio (PDR) of nodes configured with various spreading factors (SF) settings, specifically

SF values of 7, 9, and 10. The findings indicate that increasing the SF leads to improved PDR values. Additionally, a distance-dependent decrease in PDR was observed as the distance between nodes increased. As illustrated in Fig. 10., SF 10 achieved the highest PDR across all tested distances. Specifically, at 300 meters, the PDR was 55% for SF 7, which dropped to 18% to 1,000 meters. In contrast, at an SF value of 10, the PDR reached 97% at 400 meters, significantly outperforming SF 7. This experiment confirmed that elevating the spreading factor (SF) enhances both transmission range and data delivery performance. However, it is important to note that while increasing the SF improves PDR, it also contributes to increased latency.

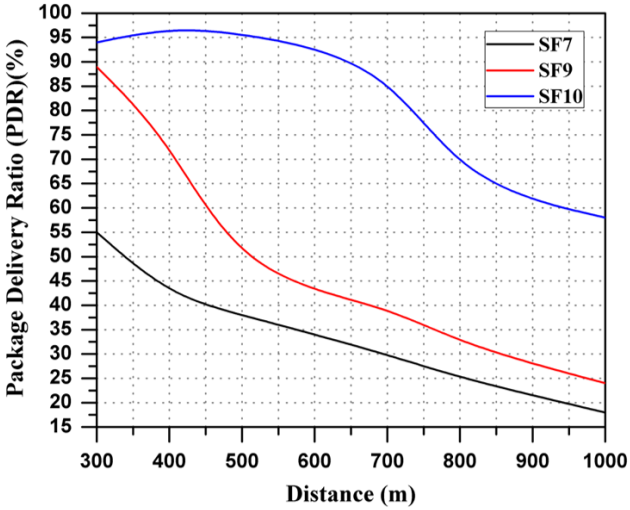

Fig. 10. The PDR values at various distances across different SF configurations.

The packet delivery ratio, or PDR, may be derived from equation (8).

$$PDR = \frac{P_{success}}{P_{sends}} \tag{8}$$

$P_{success}$ represents the successful transmission of packets, while P_{sends} represents the total number of packets sent and provides network data collected from all sending nodes.

Fig. 11. illustrates the installation layout for the transmission equipment that links the air quality LoRa station, the LoRa repeater, and the LoRa gateway, with a total installation distance of approximately 1.7 kilometers. The LoRa gateway is situated at the Mae Chan Subdistrict Administrative Organization in the Mae Chan District of Chiang Rai Province, Thailand.

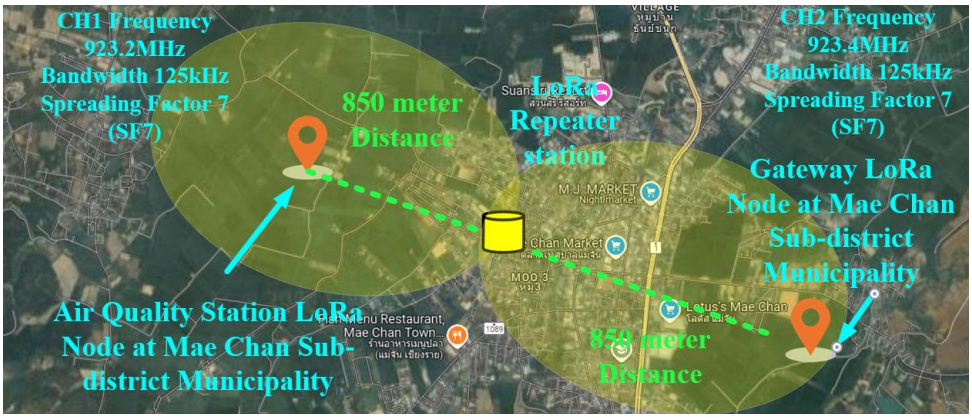

Fig. 11. illustrates the transmission distance map from the air quality LoRa station to the LoRa gateway and installation site.

When implementing a mesh transmission model, it is essential to consider the time-on-air value associated with each data packet. This value tends to increase with greater distances or a higher number of transmissions. The forthcoming experiment will focus on measuring the duration of data transmission in a two-hop system that includes an air quality LoRa node, a LoRa repeater, and a LoRa gateway. This investigation will involve varying the bandwidth and spreading factor (SF) during the data transmission process. Fig. 12. presents the experimental findings related to airtime.

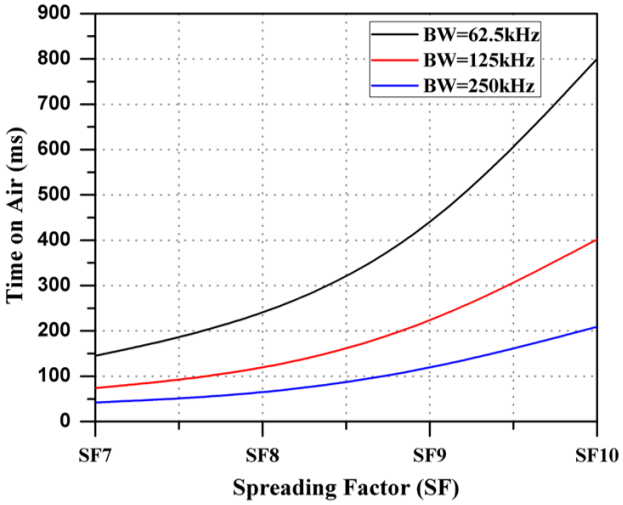

Fig. 12. Duration of transmission under various spreading factors and bandwidth configurations.

Fig. 12. illustrates the effects of different bandwidth (BW) and spreading factors (SF) on the duration of wireless data transmission, commonly referred to as time on air. The study aims to evaluate how SF and BW influence airtime. It was observed that a larger SF, combined with a smaller BW, correlates with an increased airtime period. Specifically, the airtime duration was measured at 42 ms when the spreading factor (SF) was set to 7 and the bandwidth (BW) was 250 kHz. In contrast, increasing the SF to 10 while reducing the bandwidth to 62.5 kHz resulted in a significant increase in airtime, extending the duration to 800 ms.

5. Results and Discussion

The experimental results demonstrate the effectiveness of the proposed LoRa-based repeater system in extending communication range for air quality monitoring. Pollutant data collected over a day confirmed that the sensing node reliably detected and transmitted multiple gas and particulate concentrations to the gateway. Specifically, Fig. 13(a) illustrates daily measurements of CO_2, while Fig. 13(b) presents NO_2 concentrations, and Fig. 13(c) details SO_2 measurements collected within the same sampling period. Dust concentrations were also successfully captured, with Fig. 14(a) highlighting recorded PM2.5 and PM10 levels. These results validate that the system's sensor integration supports continuous and accurate monitoring of key environmental pollutants.

In addition to pollutant detection, the system's communication performance was assessed. Fig. 14(b) and 14(c) depict the measured Received Signal Strength Indicator (RSSI) and Signal-to-Noise Ratio (SNR) between the monitoring station and the LoRa gateway. The RSSI values fluctuated between –84 dBm and –92 dBm when measured between the monitoring station and the repeater, while repeater-to-gateway RSSI values ranged from –69 dBm to –112 dBm. Since the SX1276 chip is capable of decoding signals down to –123 dBm at SF7, these results confirm sufficient signal margins for reliable transmission. The data also indicate that higher RSSI values correlate with stronger signal reception, demonstrating the effectiveness of the repeater in stabilizing the link under varying conditions.

The average Packet Delivery Ratio (PDR) across trials was 25% at SF7, improving to 65% at SF10 with a bandwidth of 125 kHz. However, latency increased from 42 ms at SF7 to approximately 800 ms at SF10, highlighting the inherent trade-off between spreading factors, reliability, and transmission delay. Power consumption tests showed that the solar-powered repeaters consumed less than 500 mW on average, supporting autonomous operation in remote deployments. A cost comparison further revealed that the system is approximately 30–40% less expensive than NB-IoT alternatives in similar environments, underscoring its economic feasibility for municipal-scale monitoring.

The physical implementation of the system is shown in Fig. 15, which depicts the prototype air quality monitoring station built around an ATMEGA2560 microcontroller and equipped with MQ131, MQ9, MG811, 2SH12, and PMS3003 sensors. Sensor data are transmitted to the LoRa gateway via SPI communication with the SX1276 module, while the Raspberry Pi gateway forwards collected information to the ThinkSpeak IoT platform for cloud-based storage, analysis, and visualization of both pollutant levels and power metrics.

5.1 Trade-offs Between SF, PDR, and Bandwidth

The results confirm the expected relationship between spreading factor (SF), packet reliability, and bandwidth. Higher SF values (e.g., SF10) provided stronger resilience to noise and improved PDR, achieving up to 97% at 400 m, but resulted in reduced bandwidth and increased latency. Conversely, lower SF values (e.g., SF7) supported higher data throughput but exhibited poorer reliability at greater distances. For practical applications, this implies that deployments requiring high reliability—such as health-related monitoring—should operate at higher SFs, while applications prioritizing rapid sampling may utilize lower SFs over shorter ranges.

5.2 Comparative Analysis of Existing Solutions

When compared with existing long-range IoT approaches, the proposed repeater-based design demonstrates several advantages. Duong et al. (2018) developed multi-hop LoRa protocols for linear infrastructures such as pipelines and power lines. While effective in extending coverage, their method required synchronization between nodes, increasing complexity and energy consumption. Similarly, Abrardo and Pozzebon (2019) optimized multi-hop LoRa for underground aqueducts, but their system was limited to ~200 m in obstructed conditions, demonstrating the inadequacy of star-topology LoRa networks for long-range monitoring. In contrast, the proposed repeater-enhanced system extended transmission to 1.7 km in semi-rural conditions, while maintaining lower system complexity and energy requirements compared with multi-hop and satellite solutions. Satellite backhauls, although capable of global coverage, remain prohibitively expensive and power-intensive for low-cost air quality applications.

5.3 Practical Implications and Limitations

The results indicate that incorporating a repeater into LoRa-based monitoring networks provides a practical and scalable solution for reliable long-range data transmission. An operational range of 850 m per hop was consistently achieved with stable RSSI and acceptable PDR, making the system well-suited for small municipalities, peri-urban areas, and industrial zones. Nonetheless, limitations exist. Environmental factors such as weather and interference from other devices in the 923 MHz band affected signal stability. Furthermore, while higher SF values improved reliability, they increased airtime, which could reduce scalability when multiple nodes transmit concurrently. Future enhancements may include adaptive data rate (ADR) algorithms, directional antennas to improve link budgets, and expanded hybrid energy-harvesting techniques to further increase system autonomy.

5.4 Validation Against Theoretical Models

Measured RSSI values were compared with the log-distance path loss model (reference distance = 1 m) and showed strong alignment with theoretical predictions. These findings are consistent with prior results reported by Duong et al. (2018) and Abrardo & Pozzebon (2019), thereby validating the reliability and performance of the proposed repeater-based configuration in real-world conditions.

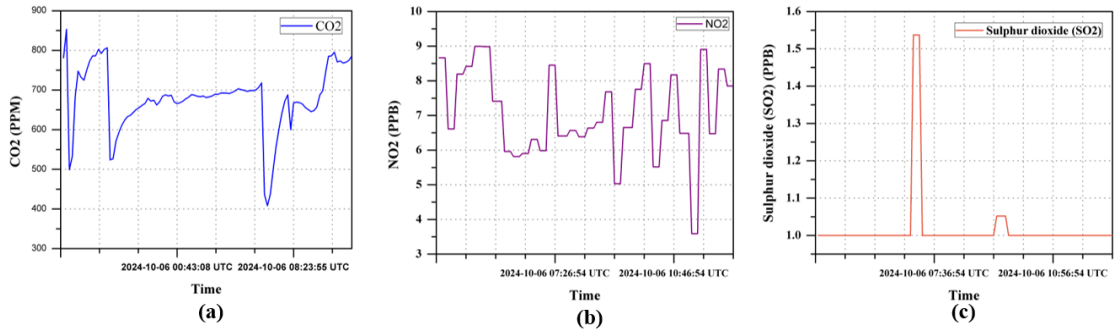

Fig.13. shows the reported (a)carbon dioxide (b) Nitrogen dioxide (c) Sulphur dioxide.

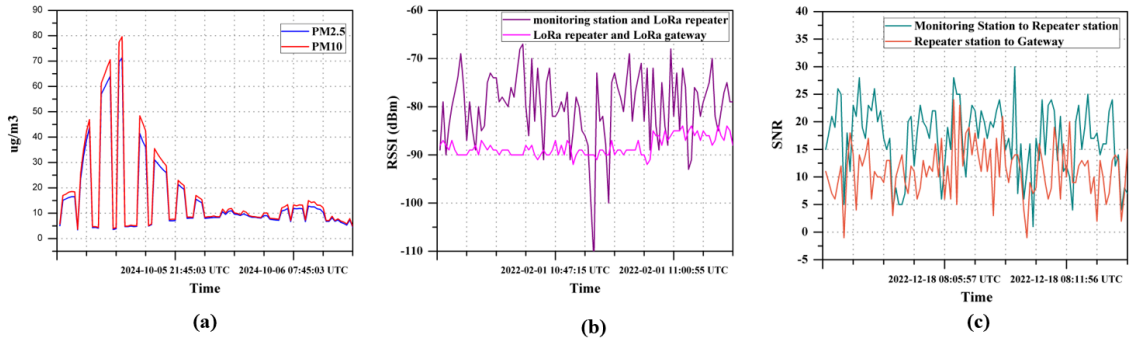

Fig.14. shows the reported (a)PM2.5 and PM10 (b) RSSI values (c) SNR values.

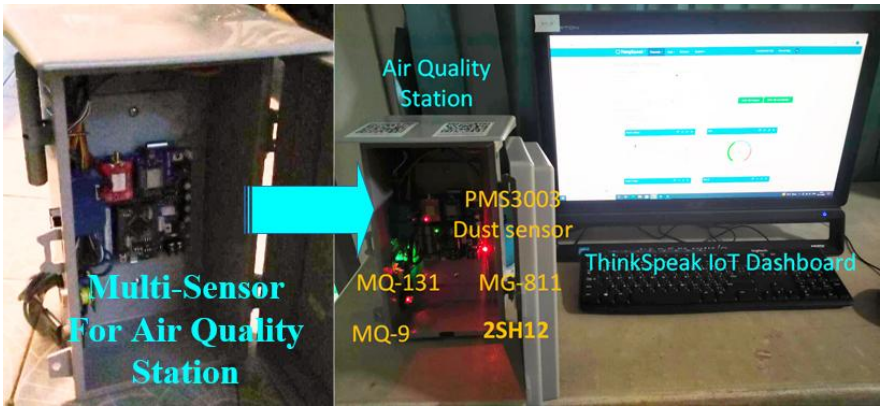

Fig. 15. depicts the prototype air quality monitoring station apparatus before its installation.

6. Conclusion

This study has demonstrated the effectiveness of a LoRa-based repeater system for extending the operational range of air quality monitoring stations. Experimental results showed that the signal strength between the monitoring node and repeater fluctuated between –84 dBm and –92 dBm, while the repeater-to-gateway RSSI ranged from –69 dBm to –112 dBm, values well above the –123 dBm sensitivity threshold of the SX1276 transceiver. The system achieved a practical operational range of 850 meters per hop, with the overall transmission distance extended to approximately 1.7 km in semi-rural deployment conditions.

In terms of reliability, the Packet Delivery Ratio (PDR) was recorded at 25% for SF7, improving to 65% at SF10 with a bandwidth of 125 kHz. Latency increased from 42 ms at SF7 to approximately 800 ms at SF10, highlighting the trade-off between throughput, reliability, and delay. Power measurements confirmed that the solar-powered repeater consumed less than 500 mW, enabling sustainable operation in remote locations. Furthermore, cost analysis indicated that

the proposed solution is 30–40% more affordable than NB-IoT deployments in comparable settings, emphasizing its economic viability.

The key contributions of this work are threefold:

1. The design and implementation of a cost-effective LoRa repeater system tailored for air quality monitoring.
2. A quantitative evaluation of system performance, including RSSI, SNR, PDR, latency, and power consumption, under real-world deployment conditions.
3. A comparative analysis with existing solutions, demonstrating that the repeater-based approach provides lower complexity and energy consumption than multi-hop alternatives while remaining significantly more cost-effective than satellite backhaul.

The practical implications of these findings are considerable. The system offers a scalable, low-cost solution for municipalities, industrial zones, and peri-urban regions, where traditional monitoring systems are economically or technically impractical. Beyond environmental monitoring, the approach can be extended to industrial automation, smart agriculture, and other IoT applications requiring reliable, long-distance data transmission.

Nonetheless, limitations remain. Environmental factors such as weather variability and interference at 923 MHz can affect link stability, and higher spreading factors, while improving reliability, increasing airtime and reduce scalability when multiple nodes operate concurrently. Future research should therefore explore adaptive data rate (ADR) algorithms, the integration of directional or high-gain antennas, and hybrid energy harvesting techniques to enhance reliability and system autonomy. Additionally, scaling the system to multi-repeater networks and testing under dense urban conditions would further validate its applicability for smart city deployments.

In conclusion, this research advances the field of IoT-based environmental monitoring by demonstrating that LoRa repeaters provide a practical, energy-efficient, and cost-effective means of extending communication range, thereby addressing one of the key challenges in achieving reliable and scalable air quality monitoring systems.

Acknowledgement

This work was supported by Chiangrai Rajabhat University and the National Research Council of Thailand, Grant No. FF68-1-021.

References

Abrardo, A., & Pozzebon, A. (2019). A multi-hop LoRa linear sensor network for the monitoring of underground environments: The case of the medieval aqueducts in Siena, Italy. *Sensors, 19*(2), 402. https://doi.org/10.3390/s19020402

Adelantado, F., Vilajosana, X., Tuset-Peiró, P., Martínez, B., Melia-Seguí, J., & Watteyne, T. (2017). Understanding the limits of LoRaWAN. *IEEE Communications Magazine, 55*(9), 34–40. https://doi.org/10.1109/MCOM.2017.1600613

Akyildiz, I. F., & Jornet, J. M. (2010). The Internet of nano-things. *IEEE Wireless Communications, 17*(6), 58–63. https://doi.org/10.1109/MWC.2010.5675779

Belli, L., Cirani, S., Davoli, L., Ferrari, G., Melegari, L., & Picone, M. (2015). Design and deployment of an IoT application-oriented testbed. *Computer*, *48*(9), 32-40. https://doi.org/10.1109/MC.2015.253

Boonlom, K., Khonrang, J., Rungraungsilp, S., Amsdon, T., Robertson, I., & Somjit, N. (2024). Advancing in-pipe robot communication with high-speed OWC transceiver front-end circuit: Experimental insights and prospects. In *Proceedings of the 21st International Conference on Electrical Engineering/Electronics, Computer, Telecommunications and Information Technology (ECTI-CON)* (pp. 1–6). IEEE. https://doi.org/10.1109/ECTI-CON60892.2024.10595010

Boonlom, K., Pratumvinit, T., & Akkaraekthalin, P. (2009). A compact microstrip two-layers bandpass filter using improved interdigital-loop resonators. In *Proceedings of the 2009*

IEEE International Symposium on Radio-Frequency Integration Technology (RFIT) (pp. 367–370). IEEE. https://doi.org/10.1109/RFIT.2009.5383685

Boonlom, K., Viratikul, R., Robertson, I. D., Amsdon, T., Chudpooti, N., & Somjit, N. (2023). Illumination and bandwidth control circuit for LED optical wireless transmitter driver integrated with passive second-order equaliser for pipe robot application. In *Proceedings of the 2023 Research, Invention, and Innovation Congress: Innovative Electricals and Electronics (RI2C)* (pp. 1–5). IEEE. https://doi.org/10.1109/RI2C60382.2023.10356036

Boonlom, K., Chomtong, P., Zhang, W., Amsdon, T. J., Oberhammer, J., Robertson, I. D., & Somjit, N. (2024a). Advanced studies on optical wireless communications for in-pipe environments: Bandwidth exploration and thermal management. *IEEE Access, 12*, 80607–80632. https://doi.org/10.1109/ACCESS.2024.3410465

Boonlom, K., Khonrang, J., Siri, A., & Klinhnu, J. (2021). The design and development of microgrid electrical power supply for seismo sensor with an artificial perceptron neural network. *Review of International Geographical Education (RIGEO), 11*(9), 2711–2721. https://doi.org/10.48047/rigeo.11.09.238

Boonlom, K., Khonrang, J., Amsdon, T., Robertson, I., & Somjit, N. (2022). Active pre-equalizer for broadband optical wireless communication integrated with RF amplifier. In *Proceedings of the 2022 Research, Invention, and Innovation Congress: Innovative Electricals and Electronics (RI2C)* (pp. 251–254). IEEE. https://doi.org/10.1109/RI2C56397.2022.9910315

Boonlom, K., Chudpooti, N., Rungraungsilp, S., Zhang, W., Amsdon, T., Oberhammer, J., & Somjit, N. (2025). Multiwavelength Optical Sensing of Water-Level Stratification in Closed Plastic Pipelines Using Signal Attenuation and CIR Analysis. *IEEE Sensors Journal*. https://doi.org/10.1109/JSEN.2025.3598923

Brunekreef, B., & Holgate, S. T. (2002). Air pollution and health. *The Lancet, 360*(9341), 1233–1242. https://doi.org/10.1016/S0140-6736(02)11274-8

Castell, N., Dauge, F. R., Schneider, P., Vogt, M., Lerner, U., Fishbain, B., … Bartonova, A. (2017). Can commercial low-cost sensor platforms contribute to air quality monitoring and exposure estimates?. *Environment International, 99*, 293–302. https://doi.org/10.1016/j.envint.2016.12.007

Cohen, A. J., Brauer, M., Burnett, R., Anderson, H. R., Frostad, J., Estep, K., … Forouzanfar, M. H. (2017). Estimates and 25-year trends of the global burden of disease attributable to ambient air pollution: An analysis of data from the Global Burden of Diseases Study 2015. *The Lancet, 389*(10082), 1907–1918. https://doi.org/10.1016/S0140-6736(17)30505-6

European Environment Agency. (2021). *Air quality in Europe — 2021 report (EEA Report No. 10/2021)*. European Environment Agency. https://www.eea.europa.eu/publications/air-quality-in-europe-2021

Greenpeace Southeast Asia. (2022, June 2). *The burden of air pollution in Thailand 2021 report. Greenpeace Southeast Asia*. https://www.greenpeace.org/southeastasia/publication/45439/the-burden-of-air-pollution-in-thailand-2021report/

Hossain, M. S., & Muhammad, G. (2016). Cloud-assisted industrial internet of things (iiot)–enabled framework for health monitoring. *Computer Networks, 101*, 192-202. https://doi.org/10.1016/j.comnet.2016.01.009

Industrial Air Pollution. (2014, April 29). *Industrial air pollution has high economic cost. European Environment Agency*. https://www.eea.europa.eu/media/newsreleases/industrial-air-pollution-has-high

Jawad, H. M., Nordin, R., Gharghan, S. K., Jawad, A. M., & Ismail, M. (2017). Energy-efficient wireless sensor networks for precision agriculture: A review. *Sensors, 17*(8), 1781. https://doi.org/10.3390/s17081781

Jayaraman, P. P., Yavari, A., Georgakopoulos, D., Morshed, A., & Zaslavsky, A. (2016). Internet of Things platform for smart farming: Experiences and lessons learnt. *Sensors, 16*(11), 1884. https://doi.org/10.3390/s16111884

Khonrang, J., Somphruek, M., Duangnakhorn, P., Siri, A., & Boonlom, K. (2023). Experimental and case studies of long-distance multi-hopping data transmission techniques for wildfire sensors using the LoRa-based mesh sensor network. *International Journal of Electronics and Telecommunications, 69*(1), 419–424. https://doi.org/10.24425/ijet.2023.144378

Kitchin, R. (2014). The real-time city? Big data and smart urbanism. *GeoJournal, 79*(1), 1–14. https://doi.org/10.1007/s10708-013-9516-8

Ksentini, A., & Nikaein, N. (2017). Toward enforcing network slicing on RAN: Flexibility and resources abstraction. *IEEE Communications Magazine, 55*(6), 102–108. https://doi.org/10.1109/MCOM.2017.1601119

Kumar, P., Skouloudis, A. N., Bell, M., Viana, M., Carotta, M. C., Biskos, G., & Morawska, L. (2016). Real-time sensors for indoor air monitoring: Reliability and end-user perspective. *Environment International, 94*, 317–326. https://doi.org/10.1016/j.scitotenv.2016.04.032

Li, S., Da Xu, L., & Zhao, S. (2015). The internet of things: A survey. *Information Systems Frontiers, 17*(2), 243–259. https://doi.org/10.1007/s10796-014-9492-7

Lin, K., Chen, M., Deng, J., Hassan, M. M., Fortino, G., & Li, W. (2017). Enhanced fingerprinting and trajectory prediction for IoT localization in smart buildings. *IEEE Transactions on Automation Science and Engineering, 14*(3), 1294–1307. https://doi.org/10.1109/TASE.2016.2543242

Magno, M., & Benini, L. (2014, October). An ultra low power high sensitivity wake-up radio receiver with addressing capability. In *2014 IEEE 10th International Conference on Wireless and Mobile Computing, Networking and Communications (WiMob)* (pp. 92-99). IEEE. https://doi.org/10.1109/WiMOB.2014.6962155

Morawska, L., Thai, P. K., Liu, X., Asumadu-Sakyi, A., Ayoko, G., Bartonova, A., … Williams, R. (2018). Applications of low-cost sensing technologies for air quality monitoring and exposure assessment: How far have they gone?. *Environment International, 116*, 286–299. https://doi.org/10.1016/j.envint.2018.04.018

Ndaguba, E., Cilliers, J., Ghosh, S., Herath, S., & Mussi, E. T. (2023). Operability of smart spaces in urban environments: A systematic review on enhancing functionality and user experience. *Sensors, 23*(15), 6938. https://doi.org/10.3390/s23156938

Olasupo, T., Otero, C. E., Olasupo, K. O., & Kostanic, I. (2016). Empirical path loss models for wireless sensor network deployments in short and tall natural grass environments. *IEEE Transactions on Antennas and Propagation, 64*(9), 4012-4021. https://doi.org/10.1109/TAP.2016.2583507

Popoola, O. A., Carruthers, D., Lad, C., Bright, V. B., Mead, M. I., Stettler, M. E., ... & Jones, R. L. (2018). Use of networks of low cost air quality sensors to quantify air quality in urban settings. *Atmospheric environment, 194*, 58-70. https://doi.org/10.1016/j.atmosenv.2018.09.030

Qadir, Q. M., Rashid, T. A., Al-Salihi, N. K., Ismael, B., Kist, A. A., & Zhang, Z. (2018). Low power wide area networks: A survey of enabling technologies, applications and interoperability needs. *IEEE Access, 6*, 77454–77473. https://doi.org/10.1109/ACCESS.2018.2883151

Sha, K., Wei, W., Yang, T. A., Wang, Z., & Shi, W. (2018). On security challenges and open issues in Internet of Things. *Future Generation Computer Systems, 83*, 326–337. https://doi.org/10.1016/j.future.2018.01.059

Shafique, K., Khawaja, B. A., Sabir, F., Qazi, S., & Mustaqim, M. (2020). Internet of Things (IoT) for next-generation smart systems: A review of current challenges, future trends, and prospects for emerging 5G-IoT scenarios. *IEEE Access, 8*, 23022–23040. https://doi.org/10.1109/ACCESS.2020.2970118

Vijay, P. J., Madhuri, A., Sri, G. M., & Prasad, Y. S. V. S. N. (2023, March). A Survey on IOT Based Air Pollution Monitoring System. In *2023 4th International Conference on Signal Processing and Communication (ICSPC)* (pp. 52-55). IEEE. https://doi.org/10.1109/ICSPC57692.2023.10125940

Viratikul, R., Boonlom, K., Robertson, I., Amsdon, T., Janpugdee, P., & Somjit, N. (2024). Design and evaluation of optical wireless communication systems for underwater IoT applications. In *Proceedings of the 11th International Conference on Wireless Networks*

and Mobile Communications (WINCOM) (pp. 1–6). IEEE. https://doi.org/10.1109/WINCOM62286.2024.10655875

World Health Organization. (2021). *Air pollution*. Retrieved August 20, 2023, from https://www.who.int/teams/environment-climate-change-and-health/air-quality-and-health/

Zanella, A., Bui, N., Castellani, A., & Zorzi, M. (2014). Internet of Things for smart cities. *IEEE Internet of Things Journal, 1*(1), 22–32. https://doi.org/10.1109/JIOT.2014.2306328